Electron spin resonance in EuB_6

A. V. Semeno,[1] V. V. Glushkov,[1] A. V. Bogach,[1] N. E. Sluchanko,[1] A. V. Dukhnenko,[2] V. B. Fillippov,[2] N. Yu. Shitsevalova,[2] and S. V. Demishev[1]

[1]*A.M. Prokhorov General Physics Institute, RAS, 38, Vavilov Str., Moscow 119991, Russia*

[2]*Institute for Problems of Materials Science, NAS, 3, Krzhizhanovsky Str., 03680 Kiev, Ukraine*

(Received 11 July 2008; revised manuscript received 2 December 2008; published 21 January 2009)

Cavity measurements of a high frequency (60 GHz) electron spin resonance (ESR) have been carried our for a single crystal of EuB_6 at temperatures 4.2–50 K in magnetic field up to 7 T, which has been aligned along [001] crystallographic direction. It is found that in the case of homogeneous magnetic field in the sample the ESR spectrum of EuB_6 is formed by a single line at all temperatures including the ferromagnetic ordering region, whereas the gradient of magnetic field in the samples induces double peak ESR structure at low temperatures. For the quantitative description of the ESR line shape we suggested an analytical approach applicable for the cavity measurements of a metal with an arbitrary value of magnetic permeability including strongly magnetic case and obtained full set of the ESR parameters, namely oscillating magnetization M_0, g factor, and linewidth. Our analysis has explained the visible resonance line shift and revealed the coincidence of the oscillating magnetization defining the resonance amplitude with the static magnetization. The anomalous growth of the linewidth below Curie temperature $T_C \approx 15$ K is observed. We argue that ESR in EuB_6 is not considerably affected by either interaction with the spin polarons or the magnetic phase separation and reflects merely the oscillation of the Eu^{2+} localized magnetic moments, which can be well understood within mean-field approximation.

DOI: 10.1103/PhysRevB.79.014423 PACS number(s): 71.20.Eh, 71.27.+a, 71.38.−k, 75.30.−m

I. INTRODUCTION

EuB_6 is a ferromagnetic strongly correlated metal with Curie temperature $T_C \approx 15$ K.[1,2] Magnetic properties of EuB_6 are supposed to originate mostly from the localized Eu^{2+} ions having the effective magnetic moment $\mu_{\text{eff}} \approx 7.9\mu_B(S=7/2)$.[1] This material also attracts attention as possessing a complicated magnetic transition structure[1,2] together with the "colossal" magnetoresistive effect,[1] which is presumably caused by strong interaction of the itinerant carriers to the localized magnetic moments. However, neither the mechanism of the ferromagnetic interaction (see the discussion in Ref. 3) nor the origin of strong negative magnetoresistance in the vicinity of the magnetic transition is completely clarified up to now.

As long as electron spin resonance (ESR) may serve as a powerful tool for examining of the interaction between the magnetic moments and the itinerant carriers,[4] numerous attempts have been performed to utilize this technique for EuB_6.[5–10] The results of these studies look very controversial, e.g., the linewidth values measured in Refs. 5–10 exhibit considerable discrepancy even at high temperatures and the difference in the observed linewidth reaches several times at helium temperatures. Additionally, some authors report a splitting of the resonance line below T_C, which may be a consequence of the magnetically inhomogeneous ground state.[5,6,10] Thus, the low temperature ESR spectrum structure is not completely clear both on qualitative and quantitative levels.

The present work is aimed on shedding more light on ESR problem in EuB_6. We argue that the aforementioned difficulties result from (i) the inhomogeneity of the magnetic field in the sample, which may vary in different experiments, and (ii) the methodological problem of quantitative description of the ESR line shape in strongly magnetic material. A procedure of the ESR data analysis, which allows finding the microscopic magnetic permeability parameters, is suggested. The results are discussed in the framework of the existing models of magnetic ordering in EuB_6.

II. EXPERIMENTAL DETAILS

In our experiments we used high quality single crystals of EuB_6. The structure of the samples and absence of the technological impurities were controlled by x-ray diffraction and microchemical analytical methods. The crystals studied by ESR were also examined in detail by means of the galvanomagnetic, thermoelectric, and magnetic measurements.[11] The results of this investigation are in good agreement with the data available in literature for high quality single crystals, including the observation of the complex magnetic transition structure consisting of two consequent transitions at $T_{C1} \approx 15.6$ K and $T_{C2} \approx 13.9$ K in the resistivity temperature dependence. High residual resistivity ratio $\rho(300\text{ K})/\rho(2\text{ K}) > 30$ and good agreement of transition temperatures T_{C1} and T_{C2} with reported values[2] provide a convincing evidence for the high quality of EuB_6 crystal studied in our work. More details about the mentioned physical properties of the samples can be found elsewhere.[11]

Magnetic resonance measurements were carried out with the help of original cavity magneto-optical spectrometer. In our setup the cylindrical transmitting cavities operating at TE_{01n} modes ($n=1,2,4$) and covering the frequency range 40–100 GHz were located in the cryostat with the superconducting magnet. The magnetic field **H** was parallel to the cavity axis and varied in the experiment up to 7 T. The construction of the setup allowed providing experiments in the temperature range 1.8–300 K with the accuracy of tempera-

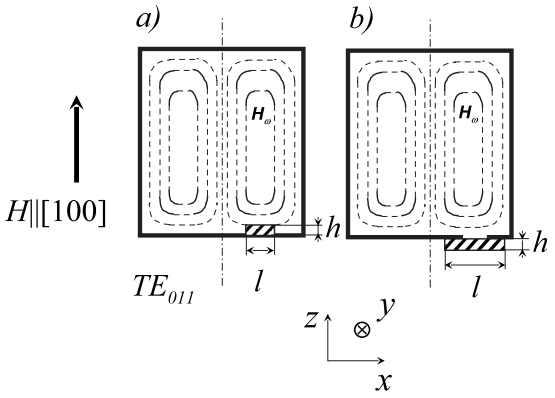

FIG. 1. Experimental geometries for ESR measurements of EuB_6. (a) Standard scheme of ESR experiment. (b) The scheme, which allows avoiding the effect of magnetic field inhomogeneity.

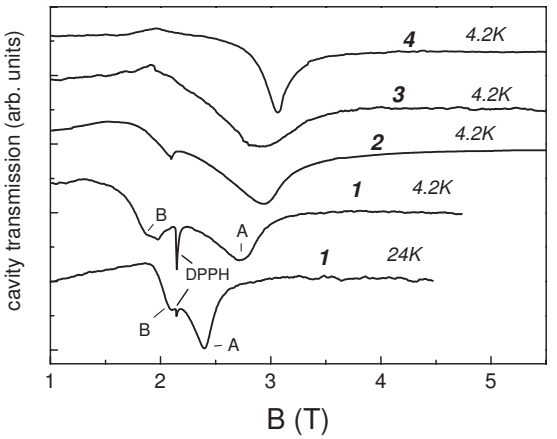

FIG. 2. ESR measurements for different geometries of experiment in EuB_6 at $f=60$ GHz. Curves 1–3 correspond to the standard scheme. Curve 1—Almost cubic sample ($l \sim h$). Curve 2—Plate sample ($l \approx 5h$). Curve 3—Plate sample ($l \approx 9h$). Curve 4 corresponds to the geometry with excluded magnetic field inhomogeneity.

ture stabilization for $T<50$ K better than 0.01 K. A set of backward wave oscillators was used as the sources of microwave radiation. Additional information about spectrometer can be found in Ref. 12. In the present paper we describe experiments carried out in 60 GHz TE_{011} cavity having the quality factor $Q \approx 6000$. The external magnetic field has been aligned along the [001] crystallographic direction of the EuB_6 single crystal. In order to obtain good electric contact between the metallic EuB_6 sample and the cavity the sample was fixed by a highly conducting glue. To apply the procedure of the baseline subtraction and absolute calibration of the ESR absorption line (see Sec. V) as well as to account correctly the demagnetization effect the temperature dependence of the loaded cavity quality factor together with the temperature and field dependences of dc resistivity and magnetization have been studied on the same crystal. The technique used for the galvanomagnetic and magnetic measurements was identical to the one applied in Ref. 11.

III. INFLUENCE OF THE INHOMOGENEITY OF THE MAGNETIC FIELD ON THE ESR SPECTRUM IN EuB_6

High value of the magnetization of EuB_6 at low temperatures ($M_{sat} \approx 7\mu_B$) (Ref. 11) suggests strong demagnetization effect and related magnetic field inhomogeneity in the sample. To test the influence of the magnetic field inhomogeneity on the ESR spectrum we have first used the experimental geometry shown in Fig. 1(a). Several plate samples of different shape characterized by the length l and the height h have been studied. It is found that the change in the ratio l/h strongly affects the measured ESR line (Fig. 2). When the sample shape was close to cube ($l/h \sim 1$) the ESR spectrum consisting of two lines A and B is observed (curves 1 in Fig. 2). The reduction in the ratio l/h to $l/h \approx 5$ damps the amplitude of the line B (curve 2 in Fig. 2). However, the ESR line remains considerably broadened (curve 3 in Fig. 2) even for the value $l/h \approx 9$ corresponding to a single resonance.

Importantly, that in the case $l/h \sim 1$ the line B appears at temperatures much higher than T_C (Fig. 2) so its origin is not related to the onset of the ferromagnetic order. It is worth noting that EuB_6 possesses metallic conductivity and thus the possible effects of electric field for the studied geometry (Fig. 1) should be weak as in usual metals.[4] The absence of the macroscopic technological inhomogeneities at the surface of the studied sample has been checked by means of microchemical analysis. This method has not revealed any macroscopic inhomogeneities confirming high quality of the sample. Moreover, various kinds of the sample surface preparations have been checked, including several roughnesses of mechanical polishing as well as different regimes of the chemical etchings. All experiments with different surface treatments have provided results identical to those presented above. Therefore it is possible to conclude that the difference in ESR spectra shown in Fig. 2 is caused by the change in the sample shape. It was established previously that the difference of the resonance fields for the modes A and B scales with the sample magnetization.[12] This fact together with the observed shape effect (Fig. 2) favors the explanation of the complex ESR spectrum structure in EuB_6 just by the presence of the gradient of magnetic field in the sample. In addition, the magnitude of the splitting of the lines A and B is close to the value of the demagnetization field for a thin plate (for example, the demagnetization field is about ≈ 1 T at $T=4.2$ K). This fact may be considered as an additional argument supporting the suggested explanation of the double peak ESR structure by macroscopic gradient of magnetic field in the sample. The detailed study of this phenomenon in EuB_6 is the subject of the separate work and will be published elsewhere.

The above consideration shows that for correct ESR analysis it is crucial to exclude the influence of the magnetic field inhomogeneity in the sample. For this purpose we have applied the following measuring procedure. A thin copper foil with a hole located at the maximal oscillating magnetic field position is used as the endplate of the cavity. The plate of EuB_6 crystal with the ratio $l/h \approx 7 (h \approx 0.5$ mm) is attached to the foil from the outside so the central part of the sample closes the hole with the diameter $d \approx 1.5$ mm [Fig.

1(b)]. In this case only the resonance from the central part of the sample can be measured and therefore it is sufficient to consider the homogeneous demagnetization field similar to the case of an infinite plate: $H=H_e-4\pi M$, where H_e is external magnetic field. The demagnetization effect from the oscillating part of magnetization is negligible because the skin depth ($\delta\approx 1.4$ μm at $T=4.2$ K and $\delta\approx 7.2$ μm at room T) is much smaller than the hole size.[13] It is worth noting that analogous methods were applied earlier[14,15] for the "large" samples, in which sizes are comparable to or exceed the cavity size. For example, in Ref. 14 a thin ferromagnetic foil was used as a cavity endplate, and in Ref. 15 a ferromagnetic rod with gold covered ends was put along the cylindrical coaxial cavity axis. However, to our best knowledge, the experimental geometry with a sample having size much smaller than the cavity dimension [Fig. 1(b)] has not been used up to now. The result of the application of the described experimental scheme [Fig. 1(b)] is illustrated by curve 4 in Fig. 2. It is visible that the absorption line becomes considerably narrower having different shapes and positions as compared to the geometry shown in Fig. 1(a). The same experiment done with different hole size ($d\approx 1$ mm) gave the same line shape and linewidth although the losses in the resonance maximum were more than twice lower than in the previous case. In our opinion the presented experiments explain the aforementioned discrepancy in the linewidth values reported earlier.[5–9]

As we will show in Sec. IV, for the homogeneous demagnetization effect it is possible to suggest the correct procedure of the ESR line shape analysis. Therefore in the present work we will report results corresponding to the experimental geometry shown in Fig. 1(b).

IV. ANALYSIS OF THE MAGNETIC RESONANCE LINE SHAPE

The fundamental approach to the analysis of the magnetic resonance in metals was developed more than 50 years ago.[14,16,17] It is known that the cavity losses caused by a metallic sample may be described using equation[18]

$$Q_{\text{sample}}^{-1}=\frac{1}{2}\text{Re}\left(\frac{i\mu\omega}{\sigma}\right)^{1/2}|H_\omega|^2\sim \text{Re}(-i\mu R)^{1/2}, \tag{1}$$

where σ and R are the conductivity and the sample resistance, respectively, $\mu=\mu_1-i\mu_2$ is the complex magnetic permeability, ω denotes the frequency of microwave radiation, Q_{sample} is a contribution from the sample to the cavity Q factor and H_ω is for oscillating magnetic field at the sample surface. The interaction of microwaves with the magnetic moments may be described by Bloch-Bloembergen (BB) or Landau-Lifshitz (LL) phenomenological equations. General solution of these equations is a matrix of the magnetic permeability coefficients,[13] which has the following fundamental structure:

$$\begin{vmatrix} \mu & i\mu_\alpha & 0 \\ -i\mu_\alpha & \mu & 0 \\ 0 & 0 & 1 \end{vmatrix}. \tag{2}$$

However, there is no general agreement about the best representation of the matrix coefficients μ and μ_α and several phenomenological models may be used to find these quantities. In the BB case the permeability matrix coefficients acquire the form[17]

$$\mu=\mu_1-i\mu_2=1+4\pi\chi_1-4\pi i\chi_2 = 1+\frac{4\pi\gamma^2M_0H}{\gamma^2H^2+[i\omega+(1/T_2)]^2}, \tag{3a}$$

$$\mu_\alpha=\mu_{\alpha1}-i\mu_{\alpha2}=4\pi\chi_{\alpha1}-4\pi i\chi_{\alpha2} = 1+\frac{4\pi\gamma M_0[i\omega+(1/T_2)]}{\gamma^2H^2+[i\omega+(1/T_2)]^2}, \tag{3b}$$

where γ is the gyromagnetic ratio, T_2 is the transverse relaxation time, M_0 stands for the oscillating part of the sample magnetization, and H is static magnetic field in the sample, which in the case of a thin plate equals $H=H_e-4\pi M_{\text{exp}}$ where M_{exp} is static magnetization and H_e is the external magnetic field. The analogs LL expression is given by[17]

$$\mu=\mu_1-i\mu_2=1+4\pi\chi_1-4\pi i\chi_2 = 1+\frac{4\pi\gamma M_0[\gamma H+\alpha(i\omega+\alpha\gamma H)]}{\gamma^2H^2+[i\omega+\alpha\gamma H]^2}, \tag{4a}$$

$$\mu_\alpha=\mu_{\alpha1}-i\mu_{\alpha2}=4\pi\chi_{\alpha1}-4\pi i\chi_{\alpha2} = 1+\frac{4\pi\gamma\omega M_0}{\gamma^2H^2+[i\omega+\alpha\gamma H]^2}, \tag{4b}$$

where α is the dissipation parameter. The fundamental symmetry of the considered problem demands the inclusion of the negative part of the spectra into expressions [Eqs. (3) and (4)] so thus the susceptibility $\chi_1(\chi_2)$ in Eqs. (3) and (4) should be an odd (even) function of the frequency ω. In order to obtain such functions it is necessary to add to the initial susceptibilities of Eqs. (3) and (4) antisymmetric (symmetric) functions, respectively. This transformation changes the expressions for the coefficients of the permeability matrix, so the corresponding equations are denoted below as modified Bloch-Bloembergen (mBB) and Landau-Lifshitz (mLL) expressions.

Another type of symmetric formula for the diagonal component μ was suggested by Garstens[19,20]

$$\mu=\mu_1-i\mu_2=1+4\pi\chi_1-4\pi i\chi_2, \tag{5a}$$

$$\chi_1=\chi_0\left\{\frac{1+\dfrac{\omega_0^2\tau^2}{(1+\omega_0^2\tau^2+\omega^2\tau^2)}}{(1+\omega_0^2\tau^2+\omega^2\tau^2)-\dfrac{4\omega_0^2\omega^2\tau^4}{(1+\omega_0^2\tau^2+\omega^2\tau^2)}}\right\}, \tag{5b}$$

$$\chi_2=\frac{1}{2}\chi_0\omega\tau\left(\frac{1}{1+(\omega_0-\omega)^2\tau^2}+\frac{1}{1+(\omega_0+\omega)^2\tau^2}\right), \tag{5c}$$

where χ_0 is the magnetic susceptibility, τ is the relaxation time, and $\omega_0=\gamma B$ is the resonant frequency. It is visible that Garstens (G) expression corresponds to the known Debye formula in the limit of zero magnetic field.[19,20]

Unfortunately, the off-diagonal matrix element μ_α was not obtained in the original works.[19,20] Therefore, in order to test the applicability of this approach we have followed an analogy with the mBB and mLL cases, which implies $\chi_\alpha \approx \chi$ for physically reasonable parameters. Thus we use for $\mu_\alpha = 4\pi\chi_{\alpha 1} - 4\pi\chi_{\alpha 2}$ in the G case the expressions: $\chi_{\alpha 1} = \chi_1$ and $\chi_{\alpha 2} = \chi_2$, where χ_1 and χ_2 are identical to those in Eq. (5).

In order to apply the above microscopic expressions for the magnetic permeability to the calculation of the cavity losses it is essential to make one more step, which is often missed. Our speculation is based on the ideas initially suggested by Young and Uehling.[17] In the case of electromagnetic wave propagation in an isotropic system (e.g., in free space) the incident wave may be considered as a sum of the two circularly polarized waves. The losses of each of these waves can be calculated independently using Eq. (1) with the values of the permeability for two opposite circular polarizations, $\mu_+ = \mu + \mu_\alpha$ and $\mu_- = \mu - \mu_\alpha$,[13] and the total losses are the sum of the losses of these two waves. However, in the case of the cylindrical cavity, which is used in our experiment, one should take into account that the oscillating magnetic field vectors $\mathbf{H}_\omega$ in the eigenmode are parallel to the radii of the cavity endplate. The oscillating magnetic field causes the oscillating magnetic induction in the sample in the perpendicular to $\mathbf{H}_\omega$ direction due to the hydrotropic effect represented by the permeability tensor [Eq. (2)]. In the other words, if an incident wave is linearly polarized, the reflected wave in free space must contain an oscillating orthogonal component. For example, this effect may induce a considerable radiation damping in a high frequency coil measurements of a magnetic sample.[21] However, in contrast to Ref. 21 the modes with the oscillating magnetic field perpendicular to the oscillating magnetic field of the cavity eigenmode are forbidden and the appropriate oscillating field should be zero at the sample surface. This circumstance can be taken into account by additional boundary condition. Denoting the direction of the oscillating magnetic field along the radius of the cavity endplate as **x** and perpendicular direction in the endplate plane as **y** [see Fig. 1(b)] and using expression (2) for the permeability matrix it is possible to find the oscillating components of the magnetic induction in the sample,

$$B_{\omega x} = \mu H_{\omega x} + i\mu_\alpha H_{\omega y}, \tag{6a}$$

$$B_{\omega y} = -i\mu_\alpha H_{\omega x} + \mu H_{\omega y}, \tag{6b}$$

where $H_{\omega x}$ and $H_{\omega y}$ are the microwave magnetic fields of TE_{011} mode near the sample surface (here we assume that the sample size is sufficiently small so the magnetic field near the sample surface may be considered as homogeneous). According to the above consideration the value of the magnetic induction in the sample should be zero $B_{\omega y} = 0$ at the sample surface. Then Eq. (5) gives $H_{\omega y} = i\mu_\alpha H_{\omega x}/\mu$ and hence $B_{\omega x} = (\mu - \mu_\alpha^2/\mu)H_{\omega x}$, and finally the effective permeability in **x** direction may be obtained,

$$\mu_{\text{eff}} = \mu - \mu_\alpha^2/\mu. \tag{7}$$

The functions μ and μ_α in Eq. (7) are defined by any of the microscopic expressions considered above. We wish to emphasize that the permeability μ_{eff} should be used in the Eq. (1) to calculate the cavity losses caused by the magnetic metallic sample. It is interesting that the expression for μ_{eff} coincides with the one obtained for the case of propagation of the electromagnetic wave in the direction perpendicular to magnetization.[13] If the magnetic susceptibility appearing in Eqs. (3)–(6) is small, $\chi_1, \chi_2 \ll 1$, the effective permeability μ_{eff} reduces with the high accuracy to the ordinary permeability μ that is often assumed *a priori* in the analysis of the ESR line shape. However, when $\chi_1 > 1$, the second term in Eq. (7) dominates, and amplitude, shape, and position of the resonance are changed considerably. The elementary estimations show that the accounting of the second term in Eq. (7) may be important not only for strongly magnetic systems such as ferromagnets but also for the case of the paramagnets with a narrow resonance line. Remarkably, that for the susceptibility satisfying condition $\chi_1 \gg 1$ the spin resonance position becomes very close to the point, where the denominator of the second term in Eq. (7) becomes minimal, i.e., to the point of the first zero $\chi_1 = 0$. This condition is known to correspond to the so-called antiresonance point.[13]

Summarizing the results of this section we see that Eq. (1) where μ is replaced by μ_{eff} [Eq. (7)] together with a particular choice of the magnetic permeabilities in the Landau-Lifshitz, Bloch-Bloembergen, or Garstens forms [Eqs. (3)–(6)] provides correct description of the ESR in cavity experiment for the metallic samples with the arbitrary magnetization and relaxation parameters. The derived formulae are valid for the nondegenerate cavity modes such as TE_{01n} and for the experimental geometries eliminating the inhomogeneity of the magnetic induction in the sample [Fig. 1(b)]. In Sec. V the developed approach will be applied to the quantitative analysis of the ESR in EuB_6.

V. ELECTRON SPIN RESONANCE IN EuB_6

A. Baseline subtraction and absolute calibration of the ESR data

As long as the effective magnetic permeability at zero magnetic field is expected to be very close to unity at high frequencies, the losses of the cavity caused by the sample should be proportional to the square root of the resistance $R^{1/2}$ taken at frequency ω [see Eq. (1)]. Moreover the microwave parameters in EuB_6 are defined at the studied frequency $\omega_0/2\pi \approx 60$ GHz by Drude-type behavior,[22,23] and due to the plasma frequency ω_p is much higher than ω_0,[22,23] the deviation of microwave resistance appearing in Eq. (1) from dc resistance is negligible: $R(\omega_0) \approx R(\omega = 0)$. Therefore, in order to find the part of the cavity losses caused by the sample it is sufficient to compare the zero magnetic field temperature dependencies of the full losses of the cavity with temperature dependence of dc sample resistance.

On the other hand, full losses of the cavity loaded with the sample $1/Q_f$ are the sum of the losses of the empty cavity $1/Q_0$ and the losses caused by the sample $1/Q_{\text{sample}}$, $1/Q_f = 1/Q_0 + 1/Q_{\text{sample}}$, where Q_f, Q_0, and Q_{sample} are corresponding quality factors. Consequently, if the quality factor Q_0 of the empty cavity does not depend on temperature the losses

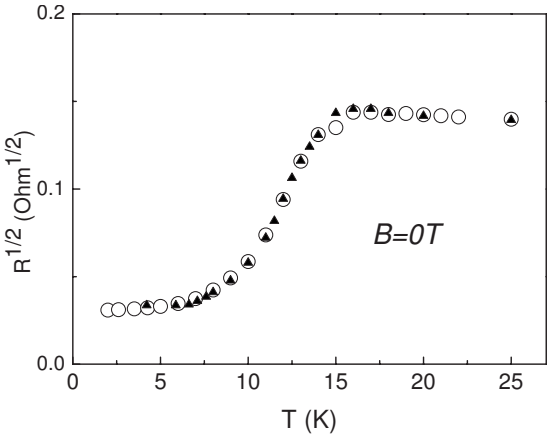

FIG. 3. Fitting of the experimental temperature dependence of $R(T)^{1/2}$ in zero magnetic field with the function $f=aQ_f^{-1}+b$. Open circles denote the square root of EuB_6 sample resistance. Triangles mark the best fit by the linear function with the parameters $a=1.54\ \Omega^{1/2}$, $b=-0.581\ \Omega^{1/2}$.

related to the sample $1/Q_{\text{sample}}$ should be a linear function of the full losses of the cavity $1/Q_f$.

The fitting of experimental temperature dependence $R(T)^{1/2}$ with the function $f(T)=aQ_f^{-1}+b$ is shown in Fig. 3. The data $Q_f(T)$ were obtained as described in Sec. II. The use of the coefficients $a=1.54\ \Omega^{1/2}$ and $b=-0.581\ \Omega^{1/2}$ provides a remarkable coincidence of $f(T)$ and $R(T)^{1/2}$ for $T<25$ K, showing that in our experiments the temperature dependence of Q_0 may be neglected at sufficiently low temperatures. Thus in the range $T<25$ K the known linear function $f(T)$ together with the field dependence of the dc resistivity allows finding the sample response from the field dependences of full cavity losses and therefore experimental $R(H)$ data may serve for the correct subtraction of the background in experimental ESR spectra. Another way for finding losses related to the sample may be based simply on the fact that the magnetic permeability is close to unity far from the resonance [Eqs. (3)–(6)]. Thus, if the resonance is narrow enough and (or) measuring frequency is sufficiently high the field dependence of the resistivity alone may be used for the subtraction procedure.

Both aforementioned methods are aimed on the establishing of the relation between nonresonant part of the cavity losses caused by the sample and the field dependence of the resistance at corresponding temperatures and therefore should provide identical results. This really meets the case for $T<25$ K, but for higher temperatures the condition $Q_0(T)=\text{const}$ fails. Therefore the value of the coefficient b changes and only the second procedure may by applied. The examples of the experimental ESR spectra together with the baselines obtained from the $R^{1/2}(H)$ dependences are shown in Fig. 4. These data clearly demonstrate that the sample losses are well described by the square root of the field dependence of dc resistance except the area of the resonance line. The considered procedure provides not only the exact method of the baseline subtraction but also gives a way for the absolute calibration of the ESR spectra. According to Eq. (1) the magnetic permeability can be easily found from the ratio of the sample losses to the square root of the resistance

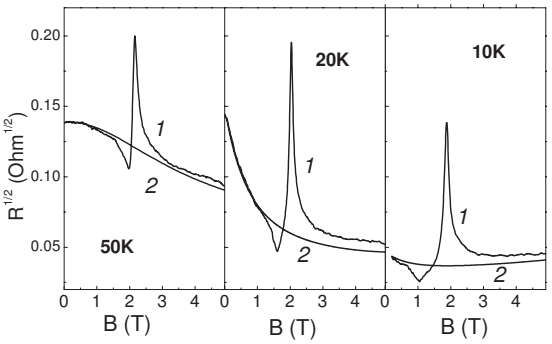

FIG. 4. Microwave sample losses in the unity of resistivity (curves 1, magnetic resonance) and dc magnetoresistance (curves 2, baseline) at various temperatures. All data are corrected to the demagnetization effect.

thus giving the ESR absorption in the units of μ. The final result of this kind of the ESR data processing is represented in Fig. 5. It is visible that ESR in EuB_6 consists of a single resonance line, which is observed at all temperatures above and below ferromagnetic transition. The value of the resonant field defined as the maximum of $\mu^{1/2}$ decreases when temperature is lowered and the resonance becomes visually broadened for $T<10$ K. When the external magnetic field is corrected to the demagnetization effect by accounting of the corresponding static magnetization data the curves $\mu(B)^{1/2}$ can be directly compared with the analytical models described in Sec. IV.

B. Simulation and fitting of the ESR line shape

We have carried out numerical simulation of the $\mu(B)$ experimental data with the help of the theoretical expressions for $\mu_{\text{eff}}(B)$ (see Sec. IV). The oscillating magnetization M_0 and the gyromagnetic ratio γ together with the parameters describing damping ($1/T_2$, τ, and α, for the BB, G and LL expressions, respectively) were used as free parameters in the fitting procedure. The value of the gyromagnetic ratio has

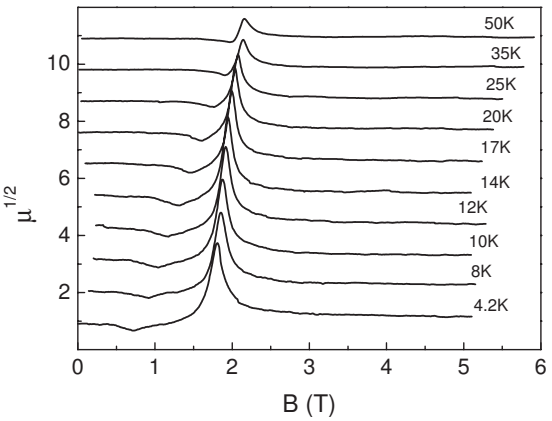

FIG. 5. Field dependencies of the magnetic permeability in EuB_6 at various temperatures. All data are corrected to the demagnetization effect. For convenience the curves are shifted consecutively along $\mu^{1/2}$ axis with respect to the curve for 4.2 K by $\Delta\mu^{1/2}=1.1$.

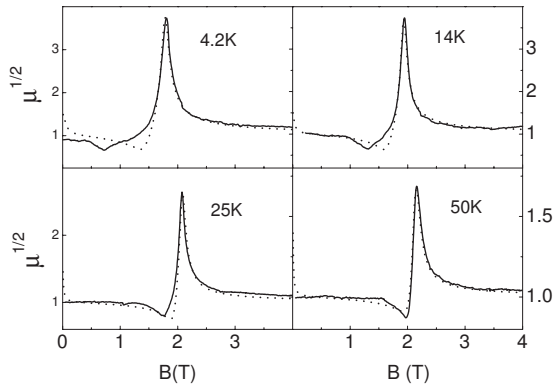

FIG. 6. Simulation of the experimental magnetic permeability curves with μ_{eff}. Solid lines—experimental data, dotted lines—fits with Garstens function. The scale of magnetic field is corrected to the demagnetization effect.

been used for further calculation of g factor while the damping parameters have been used for the evaluation of the linewidth W in the particular models. The errors of the fitting procedure applied in the vicinity of the resonance line and in high field region do not exceed 3% and reach their maximum values at lowest temperatures studied. It is found that the calculated μ_{eff} curves obtained for the different μ and μ_α functions have very similar shapes at all temperatures although the corresponding fitting parameters may vary considerably. The fitting procedure with the G function [Eq. (5)], which in our opinion provides the best representation of the line shape in the vicinity of T_C, is illustrated by Fig. 6. At temperatures $T>20$ K all theoretical expressions for μ and μ_α result in good coincidence of the simulated μ_{eff} functions with the experimental curves (Fig. 6). In the range $T<20$ K the considered approximations for μ_{eff} give good description of the experimental curves in the area close to the maximum of $\mu(B)$ as well as at higher magnetic fields. At the same time there is a considerable discrepancy between the simulated and observed $\mu(B)$ curves in the low field region and these deviations tend to increase with lowering temperature (Fig. 6).

The comparison of the experimental and simulated $\mu(B)$ data shows that the BB and LL functions give very similar line shapes and resonance parameters at all temperatures. The same is valid for the pair of mBB and mLL functions. That is why below we will compare fitting results for the mLL, LL, and G functions.

The temperature dependence of the parameter M_0 obtained with the use of the G, mLL, and LL functions together with the static magnetization taken at the resonance fields at each particular temperature is presented in Fig. 7. It is worth noting that the M_0 values corresponding to the G and mLL functions almost coincide with each other in the whole studied temperature interval. At temperatures $T>30$ K all approximations demonstrate good agreement of the calculated and measured magnetization data (Fig. 7). However upon lowering temperature the LL equation results in considerable deviation from the static magnetization dependence, while the G and mLL functions allow reproducing the static magnetization dependence in the whole temperature range.

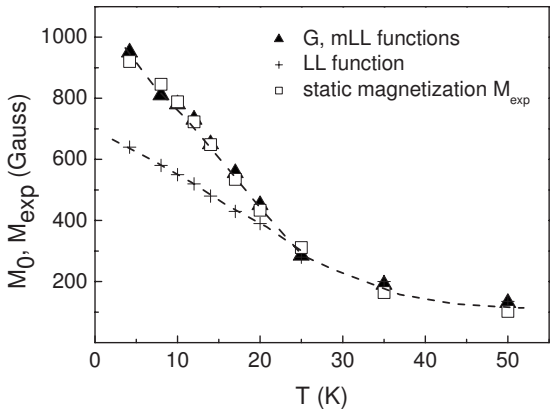

FIG. 7. Temperature dependence of the oscillating magnetization. Triangles correspond to Garstens and modified Landau-Lifshitz approaches, crosses denote Landau-Lifshitz approach. Open squares mark the static magnetization of EuB_6 taken at resonance field. Dashed lines are guides for the eyes.

Figure 8 displays the resultant g factor. In addition to the $g(T)$ values, which are defined from the μ_{eff} model, the "visible" g factor calculated from the maxima of the resonant curves in Fig. 5 is presented. Interesting that while the visible g factor changes in the temperature range 4.2–50 K by ~20%, the g factors obtained for the LL, mLL, and G functions vary only by ~3%, which is comparable with the calculation error for this parameter. Therefore the correct accounting of the cavity absorption by implying μ_{eff} [Eq. (7)] instead of μ almost eliminates the visible shift of the resonant field (Fig. 5). We wish to emphasize that accounting of the μ_{eff} is of crucial importance as long as even after the correction to the demagnetization effect the visible maximum of the $\mu(B)$ curve does not correspond to the resonance condition $\omega=\gamma B$, and naive use of the "experimental resonance filed" for the g-factor calculation in EuB_6 may be misleading.

All approximations for the functions μ and μ_α show similar temperature behavior of the linewidth although giving the

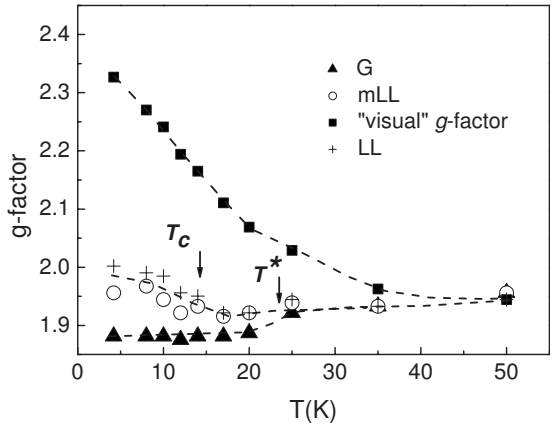

FIG. 8. Temperature dependencies of g factor. Triangles, open circles, and crosses denote the calculation results for G, mLL, LL formulae in the μ_{eff} model, respectively. Solid squares represent visible g factor calculated from the magnetic fields corresponding to μ_{eff} maxima in Fig. 5.

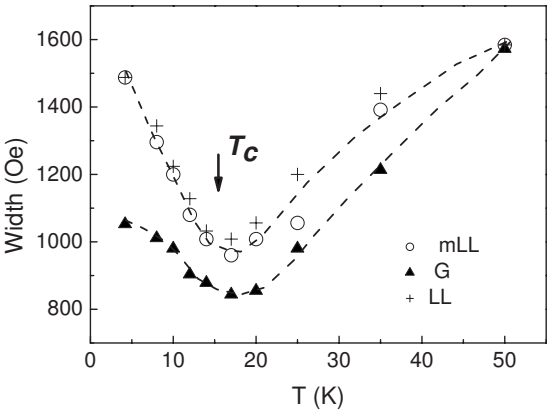

FIG. 9. Temperature dependencies of the linewidth. The legend is the same as in Fig. 8.

somewhat different values of $W(T)$ (Fig. 9). Upon lowering temperature the decrease in the linewidth is observed and the minimal value is reached in the vicinity of the Curie temperature. Further temperature decrease leads to onset of the growth of the linewidth which persists down to the lowest temperature studied (Fig. 9).

C. Discussion

In current literature it is recognized that a set of the unusual physical properties of EuB_6 originates from spin polarons, although the particular scenario of their formation may vary considerably (see Refs. 1, 2, 10, 11, and 24–27 and references cited therein). It is worth noting that the most pronounced effects of the spin polarons formation are observed in the transport properties; for example, the strong temperature-dependent transport effective-mass renormalization[11] may be mentioned as a remarkable consequence of this physical mechanism. Another widely discussed characteristic feature of EuB_6, namely, magnetic phase separation, is also explained by spin polarons.[25,27]

In the case of ESR it was supposed that the double peak structure of the spectrum, which develops at low temperatures under certain experimental conditions (Fig. 2), reflects the magnetic phase separation effect.[10,24] The strong shift of the visible g factor (Fig. 8) was also considered as caused by polaronic effect.[24] Later the positions of two ESR lines have been explained by so-called Kondo and anti-Kondo effects.[10] It is worth noting that the considered interpretation is essentially based on the observation of two ESR peaks with comparable magnitudes.[10,24] The results of the present work unambiguously show that the double peak structure is most likely a consequence of the macroscopic gradient of the magnetic induction in the sample thus putting into question the explanation based on the microscopic effect of magnetic phase separation. Indeed in all experimental situations where ESR in EuB_6 occurred in condition of homogeneous magnetic field in the sample the spectrum consisted of a single line having width noticeably less than in the case of inhomogeneous magnetic field (Figs. 3–6).

Another circumstance, which may lead to wrong interpretation, consists of the direct association of the observed resonance curves with the microscopic magnetic permeability $\mu(\omega,B)$ as it is done in Refs. 10 and 24. We see that the subtraction of the microscopic information from the ESR spectra in EuB_6 is not so straightforward, and it is essential to use μ_{eff} instead of μ and imply the proper absolute calibration. Therefore, when the correct procedure of the data analysis is used the strong "experimentally observed" g factor shift greatly reduces (Fig. 8). As long as strong temperature dependence of g factor is expected for Kondo and anti-Kondo effects[10] the results of the present work make this interpretation doubtful.

Another source of the artifacts may be incorrect choice of the magnetic permeability functions in the asymmetrical form [Eqs. (3) and (4)]. It is visible from Figs. 7–9 that both symmetrical and asymmetrical expressions for $\mu(\omega,B)$, which are used to find μ_{eff}, give very similar results for the g factor and the linewidth (Figs. 8 and 9), whereas the agreement of the M_0 temperature dependence with the static magnetization data is possible only for the symmetrical cases mLL and G (Fig. 7). Consequently assuming, for example, the LL form for $\mu(\omega,B)$, which does not satisfy the general symmetry of the problem, it is possible to "find" at least two comparable contributions in magnetization of EuB_6 below $\sim$25 K, where temperature dependence of the static magnetization and calculated $M_0(T)$ start to diverge (Fig. 7). Indeed, this "discrepancy" should mean that only part of the sample magnetization contributes to the magnetic resonance, and this "fact" will demand proper interpretation. On the other hand, it is well known that the magnetism of EuB_6 is the magnetism of the Eu^{2+} localized magnetic moments,[2] as long as the concentration of the charge carriers according to Hall effect measurements[11,28] is about $\sim 10^{-2}-10^{-3}$ electrons per Eu ion so their contribution to magnetization is small. Good agreement between the oscillating magnetization parameter M_0 deduced from the experiment and static magnetization M_{exp} in the frame of the model with symmetric $\mu(\omega,B)$ functions (Fig. 7) demonstrates that all Eu^{2+} magnetic moments participate homogeneously in the resonance motion at all temperatures.

The coincidence between M_0 and M_{exp} indicates that the elimination of the experimental and computational artifacts is very important for the correct interpretation of the ESR data in EuB_6. As the result it is obviously established that the general picture of the magnetic resonance in this material may be adequately described on the quantitative level within the mean-field approximation and corresponding semiclassical equations of motion for the localized magnetic moments. Summarizing results of our analysis of the ESR data it is possible to conclude that the picture of the magnetic resonance in this material may be adequately described quantitatively using the semiclassical equations of motion for the localized magnetic moments within mean-field approximation. The obtained ESR parameters should be then reexamined in view of magnetic ordering and possible spin-polaronic effects.

Let us consider first the magnetic ordering effects. In EuB_6 the magnetization at the resonant field is a smooth function of temperature and hence there are no abrupt changes in the magnetic resonance amplitude M_0 in the vicinity of the Curie temperature (Fig. 7). Apparently the mag-

netization data itself may include effects of interaction of the Eu^{2+} localized magnetic moments with charge carriers, but as long as $M_0(T)$ practically coincides with the static magnetization M_{exp}, this parameter of the magnetic resonance does not give any new information. Probably more important is the obtained temperature dependence of the g factor (Fig. 8). If the magnitude of the oscillating magnetic moments does not change, any noticeable variation in the resonant field in the mean-field approximation is impossible. This is valid even at the magnetic transition as long as the transformation of the uncorrelated spin rotation in the paramagnetic phase into coherent motion of spins in the ferromagnetic phase is described by the same gyromagnetic ratio γ, which does not depend on the type of spin motion.[13] Interesting, that the small changes in the g factor persist after accounting of the demagnetization effect and applying of the μ_{eff} model, although these changes are comparable with the computational errors. Namely, this parameter starts to decrease below $T^* \sim 25$ K for all model choices of $\mu(\omega,B)$ (Fig. 8) similar to the Hall coefficient behavior $R_H(T)$.[11] In the magnetically ordered state $T<T_C$ the calculated g factor saturates for the G function or starts to increase for the LL and mLL functions (Fig. 8). Thus the weak temperature variation in the g factor in the vicinity of the magnetic transition demonstrates a systematic character and therefore may reflect a real physical effect. The possible explanation of the $g(T)$ dependence is the change in the Eu^{2+} localized magnetic moments magnitude due to the screening and interaction with the free charge carriers. As long as the variation in the g factor starts at $T^*>T_C$, the obtained data may favor the scenario suggested in Ref. 25 where the formation of the spin polarons precedes the ferromagnetic transition. At the same time it is not possible to exclude some violation of the used mean-field approximation in the strongly interacting system such as EuB_6 and therefore the problem of the temperature dependence of the g factor in this material requires further theoretical treatments.

The obtained ESR linewidth $W(T)$ first decreases with lowering temperature and starts to increase below T_C (Fig. 9). The narrowing of the resonance observed with temperature lowering for $T>T_C$ may be induced by the decrease in the spin-flip scattering rate when magnetic correlations in EuB_6 become stronger. However the analogous $W(T)$ dependence is typical for ESR in normal metals with other known mechanisms of spin relaxation such as spin-electron or spin-phonon interaction.[4] In this respect it is difficult to make a definite conclusion about the origin of this effect. Both interactions of the localized magnetic moments with conduction electrons and magnon processes may contribute to observed anomaly below Curie temperature.

Transport[1,11] and optical[22,23] experiments show that the sharp transformation of carrier properties just below T_C occurs only in zero magnetic field whereas for the finite field where ESR is observed the magnetic phase transition is smooth and the distinct critical temperature is not observed (see data for $B=2$ T in Fig. 2 of Ref. 11). Although these experiments do not give the exact information about carrier relaxation time τ dependence one can expect that τ depends monotonously on temperature in the transition area. Moreover, the estimation of τ obtained from transport measurements $[\tau_{tr} \approx (4-6.5) \times 10^{-12}$ s] (Ref. 11) is of the order of magnitude lower than the relaxation time of ESR experiment $[\tau_{res} \approx (0.5-1.2) \times 10^{-10}$ s] derived from the resonance linewidth (Fig. 9). Therefore the interaction of the magnetic moments participating in the resonance with the itinerant electrons cannot be definitely treated as the only or dominating mechanism of spin relaxation. More probable that the observed low temperature increase in the $W(T)$ is governed by the establishing of the ferromagnetic order in the system and thus may be caused by the interaction of the oscillating magnetic moments with the magnons in the skin layer. Indeed, numerous observations of the ESR in metals, which undergo magnetic ordering, show that the ESR linewidth often increases below the critical temperature (see Ref. 4 and references cited therein). Although the aforementioned feature of $W(T)$ has been found in the systems where the spin polaron mechanism was not discussed[4] it is not possible to exclude that in EuB_6 the interaction with spin polarons may contribute to the observed temperature dependence of the ESR linewidth. The checking of this opportunity requires a calculation of this parameter in the framework of appropriate electron-polaron model, which has not been carried out up to now.

Before we discussed the parameters of ESR in the vicinity of maximal absorption, i.e., in a relatively high field region. Our ESR analysis shows that in the considered case of EuB_6 there is not so much space for the spin polaron effects although some minor features may reflect the interaction of the Eu^{2+} localized magnetic moments with these quasiparticles, which are considered as a main "driving force" of the numerous anomalies of magnetic and transport properties of this material. Another possible area where the presence of the spin polarons may affect ESR in EuB_6 is the low field region, where a systematic discrepancy between the calculated and observed line shape has been found at low temperatures (Fig. 6). This difficulty may be apparently overcome by considering an additional contribution to magnetic resonance absorption in the fitting equations. However, we wish to emphasize that in the cases of interaction with polarons or magnons the additional contribution should be introduced to the initial coefficient of permeability tensor μ and μ_α [Eq. (2)] and only after that the experimental permeability μ_{eff} may be calculated. The lack of the knowledge about the type of microwave response of magnetic polarons together with a number of fitting parameters in this case have prevented us from obtaining ambiguous results. Moreover, good reproducibility of the temperature dependence of calculated magnetization $M_0(T)$ for a single resonance line (Fig. 7) does not favor the accounting of the second hypothetical magnetic contribution. More likely that the used analytical expressions for the $\mu(\omega,B)$ functions are oversimplified to be exact apart of the magnetic resonance. The calculation of the expressions for $\mu(\omega,B)$, which may be suitable for the correct description of the ESR line shape in the low magnetic field area, is a real challenge for the spin polaron approach and can be considered as a prospective problem to be solved in the future theoretical studies.

VI. CONCLUSIONS

In conclusion we have shown that in conditions of a homogeneous magnetic field in the sample the electron spin

resonance in EuB_6 is formed by a single resonance line at all temperatures in the range 4.2–50 K studied including the ferromagnetic ordering region. The developed procedure of the baseline subtraction and absolute calibration of the ESR data in the cavity experiments has allowed obtaining resonant magnetoabsorption in the units of the magnetic permeability. For the quantitative description of the ESR line shape we suggest an analytical approach appropriate for the cavity measurements of a metal with an arbitrary magnetic permeability including strongly magnetic case. The checking of the suggested method has demonstrated good quality approximation of the observed ESR line shapes by the calculated ones in the resonance area. Our analysis has explained the visible resonance line shift and revealed a coincidence of the dynamical magnetization defined by the resonance amplitude with the static magnetization. The anomaly consisting in the low temperature increase in the linewidth below Curie temperature is observed. Qualitative analysis of the experimental data shows that the ESR in EuB_6 reflects the oscillation of the Eu^{2+} localized magnetic moments, which can be well understood within mean-field approximation. However some features of the g-factor temperature dependence may be definitely attributed to the presence of the spin polarons.

ACKNOWLEDGMENTS

This work was carried out in the framework of the RFBR Grants No. 07-02-00243 and No. 05-08-33463. Financial support from the INTAS Grant No. 03-51-3036 and the Program of Russian Academy of Sciences "Strongly Correlated Electrons" is acknowledged.

[1] S. Sullow, I. Prasad, M. C. Aronson, S. Bogdanovich, J. L. Sarrao, and Z. Fisk, Phys. Rev. B **62**, 11626 (2000).
[2] S. Sullow, I. Prasad, M. C. Aronson, J. L. Sarrao, Z. Fisk, D. Hristova, A. H. Lacerda, M. F. Hundley, A. Vigliante, and D. Gibbs, Phys. Rev. B **57**, 5860 (1998).
[3] J. C. Cooley, M. C. Aronson, J. L. Sarrao, and Z. Fisk, Phys. Rev. B **56**, 14541 (1997).
[4] S. Barnes, Adv. Phys. **30**, 801 (1981).
[5] W. Glaunsinger, Phys. Status Solidi B **74**, 443 (1976).
[6] S. Oseroff, R. Calvo, J. Stankiewicz, Z. Fisk, and D. Jonston, Phys. Status Solidi B **94**, K133 (1979).
[7] S. Kunii and T. Kasuya, J. Phys. Soc. Jpn. **46**, 131 (1979).
[8] J. Tarascon, J. Etourneau, J. Dance, and P. Hagenmuller, J. Less-Common Met. **82**, 277 (1981).
[9] R. R. Urbano, P. G. Pagliuso, C. Rettori, S. B. Oseroff, J. L. Sarrao, P. Schlottmann, and Z. Fisk, Phys. Rev. B **70**, 140401(R) (2004).
[10] T. Altshuler, Y. Goryunov, A. Dukhnenko, and N. Shitsevalova, JETP Lett. **88**, 224 (2008).
[11] V. V. Glushkov, A. V. Bogach, K. Gon'kov, S. Demishev, V. Ivanov, A. Kuznetzov, N. Samarin, N. Shitsevalova, K. Flachbart, and N. Sluchanko, JETP **105**, 132 (2007).
[12] S. Demishev, A. Semeno, H. Ohta, S. Okubo, I. Tarasenko, T. Ishchenko, N. Samarin, and N. Sluchanko, Phys. Solid State **49**, 1295 (2007).
[13] A. Gurevich and G. Melkov, *Magnetization Oscillations and Waves* (CRC, New York, 1996).
[14] N. Bloembergen, Phys. Rev. **78**, 572 (1950).
[15] G. Rado and J. R. Weertman, Phys. Rev. **94**, 1386 (1954).
[16] C. Kittel, Phys. Rev. **73**, 155 (1948).
[17] J. A. Young, Jr. and E. A. Uehling, Phys. Rev. **94**, 544 (1954).
[18] J. Slater, Rev. Mod. Phys. **18**, 441 (1946).
[19] M. Garstens, Phys. Rev. **93**, 1228 (1954).
[20] M. Garstens and J. Kaplan, Phys. Rev. **99**, 459 (1955).
[21] N. Bloembergen and R. V. Pound, Phys. Rev. **95**, 8 (1954).
[22] L. Degiorgi, E. Felder, H. R. Ott, J. L. Sarrao, and Z. Fisk, Phys. Rev. Lett. **79**, 5134 (1997).
[23] S. Broderick, B. Ruzicka, L. Degiorgi, H. R. Ott, J. L. Sarrao, and Z. Fisk, Phys. Rev. B **65**, 121102(R) (2002).
[24] V. V. Glushkov, A. V. Semeno, N. E. Sluchanko, A. V. Dukhnenko, V. B. Fillipov, and S. V. Demishev, Physica B **403**, 932 (2008).
[25] U. Yu and B. I. Min, Phys. Rev. Lett. **94**, 117202 (2005).
[26] P. Nyhus, S. Yoon, M. Kauffman, S. L. Cooper, Z. Fisk, and J. Sarrao, Phys. Rev. B **56**, 2717 (1997).
[27] M. L. Brooks, T. Lancaster, S. J. Blundell, W. Hayes, F. L. Pratt, and Z. Fisk, Phys. Rev. B **70**, 020401(R) (2004).
[28] S. Paschen, D. Pushin, M. Schlatter, P. Vonlanthen, H. R. Ott, D. P. Young, and Z. Fisk, Phys. Rev. B **61**, 4174 (2000).